Available online at www.sciencedirect.com
SCIENCE DIRECT®
Bioorganic & Medicinal Chemistry Letters 16 (2006) 1633–1637
Bioorganic & Medicinal Chemistry Letters

Inhibitors of epidermal growth factor receptor tyrosine kinase: Novel C-5 substituted anilinoquinazolines designed to target the ribose pocket

Peter Ballard,[a] Robert H. Bradbury,[a] Craig S. Harris,[b] Laurent F. A. Hennequin,[b] Mark Hickinson,[a] Paul D. Johnson,[a] Jason G. Kettle,[a,*] Teresa Klinowska,[a] Andrew G. Leach,[a] Remy Morgentin,[b] Martin Pass,[a] Donald J. Ogilvie,[a] Annie Olivier,[b] Nicolas Warin[b] and Emma J. Williams[a]

[a]*AstraZeneca, Mereside, Alderley Park, Macclesfield, Cheshire, SK10 4TG, UK*
[b]*AstraZeneca, Centre de Recherches, Z.I. la Pompelle, BP1050, 51689 Reims Cedex 2, France*

Received 23 November 2005; revised 2 December 2005; accepted 6 December 2005
Available online 27 December 2005

Abstract—A series of novel C-5 substituted anilinoquinazolines, selected on the basis of docking experiments and overlays with ATP in the active site of EGFR tyrosine kinase, have been prepared and found to be potent inhibitors. In vivo pharmacokinetics and disease model activity are discussed.

The receptor tyrosine kinases play a fundamental role in the aberrant signalling that is characteristic of the uncontrolled proliferation of a variety of human solid tumours. The most widely studied of all these, the epidermal growth factor receptor (EGFR) tyrosine kinase,[1] features a trans-membrane receptor with an extracellular ligand-binding domain and a helical trans-membrane region linked to an intracellular tyrosine kinase domain. EGFR is activated by homo- and heterodimerisation events following binding of epidermal growth factor (EGF) and other ligands. EGFR is part of a subfamily of four closely related receptors, three of which are catalytically active: EGFR (also known as erbB1/Her 1), erbB2 (Her 2/neu) and erbB4 (Her 4), and a fourth that is catalytically inactive, erbB3 (Her 3), which nevertheless can enter into signalling through heterodimerisation. EGFR misregulation, through, for example, overexpression and/or activating mutations, has been implicated in the development and progression of many solid tumour types[2] including lung, breast, ovary, colon, prostate and head and neck.

Inhibition of EGFR signalling has thus been identified as an attractive strategy in control of tumour proliferation, and over a decade of intense activity in the field has culminated in the discoveries and subsequent approvals of *gefitinib* **1**[3] and *erlotinib* **2**[4] for the treatment of non-small cell lung cancer following prior chemotherapeutic intervention. Both of these agents belong to the 4-anilinoquinazoline class of inhibitors, and their discovery has been extensively reviewed.[5] This chemical class of inhibitors acts via competition with ATP and the template has been heavily exploited in the search for new inhibitors of signal transduction mechanisms, both against EGFR, and other diverse kinases. The features

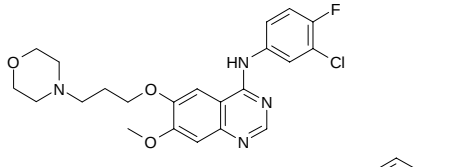

1

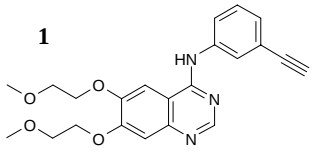

2

Keywords: EGF; Kinase; Inhibitor; Quinazoline.
* Corresponding author. Tel.: +44 1625517920; fax: +44 1625586707; e-mail: jason.kettle@astrazeneca.com

0960-894X/$ - see front matter © 2005 Elsevier Ltd. All rights reserved.
doi:10.1016/j.bmcl.2005.12.028

required for effective binding to the hinge region have been well documented.[6] By varying the aniline substitution pattern, fine-tuning of the kinase selectivity profile can be achieved. For EGFR in particular, a small, lipophilic meta-substituent is key to potent inhibition.

A second, general feature of the anilinoquinazoline template is the positioning of a solubilising side chain at C-6 and/or C-7 of the quinazoline core. These side chains act to improve physical properties and impart a more favourable pharmacokinetic profile, though they may also contribute to potency and selectivity. For potent inhibition of the erbB family, these side chains are often positioned at C-6, although side chains at both C-6 and C-7 are noted in *erlotinib* **2**, and the irreversible inhibitor *canertinib*.[7] The structures of both *erlotinib*[8] and *lapatinib*[9] bound to the catalytic domain of EGFR tyrosine kinase have been solved, confirming the positioning of these side chains at the solvent interface, and additionally, prototype 4-anilinoquinazolines have been crystallized in both CDK2 and the MAP kinase p38.[10]

Despite extensive SAR studies aimed at modifying the quinazoline core, little information was known about possible beneficial effects of substitution at C-5. Indeed, early reports with simple substituents had indicated that C-5 substitution was detrimental to activity when compared with analogous substitution at C-6 or C-7,[6] and work leading to the discovery of *gefitinib* had highlighted the perceived importance of a free CH at this position.[11] Furthermore, detailed 3D QSAR and molecular field analysis techniques have been used to suggest that the positioning of bulky groups at C-5 should not be considered.[12] However, by examining an overlay of ATP with the known binding mode of anilinoquinazolines, we postulated that substitution at C-5 with an appropriate group could lead to potent inhibitors which utilized the ribose binding pocket.[13] It was envisaged that suitably placed cyclic groups, for example, though containing heteroatoms, could mimic the interactions observed for the endogenous ligand. Figure 1 shows one such example, compound **12**, modelled into the catalytic domain of EGFR tyrosine kinase. In this model, based upon the crystal structure of EGFR tyrosine kinase in complex with *erlotinib* (PDB code 1M17), the quinazoline N-1 binds to the hinge region at Met769, with the aniline buried deep in the selectivity pocket. Also indicated is an overlay with ANP (an unreactive ATP mimic), created by overlaying the hinge binding backbone N–H and carbonyl of the EGFR tyrosine kinase structure with those of the Src kinase in complex with ANP (PDB code 2src). The quinazoline and adenosine rings are co-planar, thus positioning the ribose moiety and quinazoline C-5 substituent similarly. Based on these assumptions, synthesis of this novel class of quinazolines was undertaken, and activity with these agents subsequently confirmed.

The key C-5 bis-alkoxyquinazolines **8** were synthesised from bis-alkoxy anthranilic esters **3** according to the general procedures outlined in Scheme 1. Quinazolone ring formation was effected by treatment of the esters with formamidine acetate to give quinazolones **4**, which

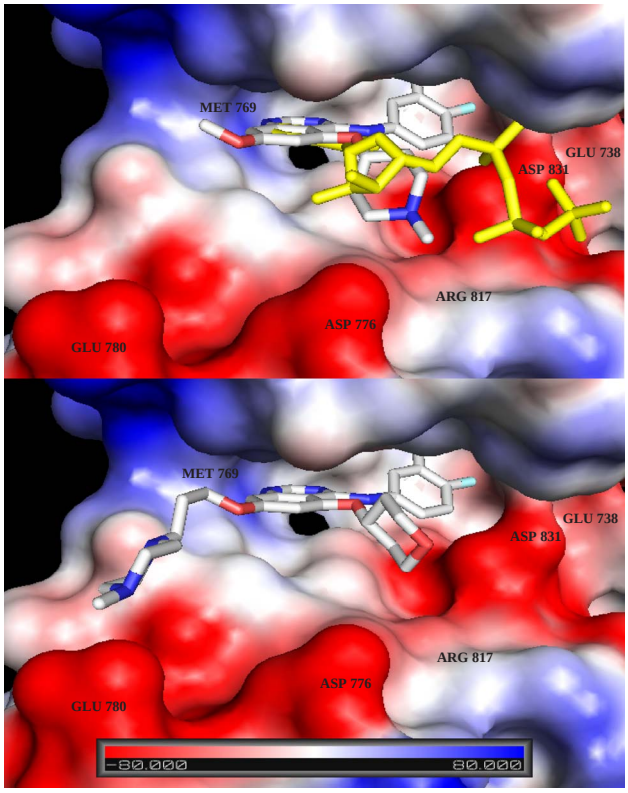

Figure 1. Compounds **12** (upper panel) and **24** (lower panel) positioned in the EGFR tyrosine kinase structure solved with *erlotinib* bound (PDB code 1m17). The molecules have the anilinoquinazoline moieties overlaid directly onto *erlotinib*, the remaining parts of the molecule shown in a representative conformation that is well ranked according to Poisson–Boltzmann-,based scoring. The protein surface is coloured according to electronic surface potential. Areas in red indicate increasing negative potential, areas in blue increasing positive surface potential. Carbon atoms are shown in grey, nitrogen in blue, oxygen atoms in red, and fluorine in pale blue. Aniline *meta*-chloro substituent is partially obscured and buried in the protein. Overlay with ATP mimic ANP (shown in yellow) is based on overlaying the hinge residues of the protein of the EGFR kinase structure with that of the Src kinase (in PDB structure 2src).

could be selectively de-alkylated at C-5 by treatment with magnesium bromide in pyridine[13,14] to give **5**. Presumably, coordination of magnesium between the C-4/5 oxygen atoms facilitates activation of the C-5 alkoxy group towards nucleophilic de-alkylation. Selective protection of the quinazoline N-3 is achieved with chloromethyl pivalate, yielding substrates **6** suitable for Mitsunobu alkylation. Treatment with DTAD/triphenyl phosphine and an appropriate alcohol furnished, after deprotection with ammonia in methanol, the corresponding quinazolones **7**. The requisite 3-chloro-4-fluoroaniline (present in both *gefitinib* and *canertinib*) was introduced via chlorination and nucleophilic aromatic substitution to give bis-alkoxy anilinoquinazolines **8**. Additionally, as outlined in Scheme 2, homologation at C-7 could be achieved by deprotection of the C-7 benzyl group in **9** with TFA, followed by alkylation of 7-hydroxyquinazoline **10** with 2-methoxyethyl bromide to yield **23**, or a basic side chain introduced by a two-step sequence to yield piperazine analogue **24**, via **11**.

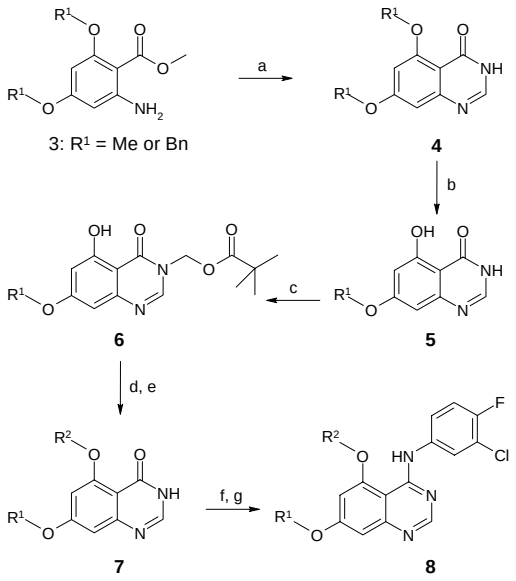

Scheme 1. Synthesis of bis-alkoxy anilinoquinazolines **8**. Reagents and conditions: (a) formamidine acetate, 2-methoxyethanol, 120 °C, 64–88%; (b) $MgBr_2$, pyridine, reflux, 93–99%; (c) NaH, chloromethyl pivalate, DMF, 0–25 °C, 67–93%; (d) DTAD, R^2-OH, Ph_3P, DCM, 70–90%; (e) 7 N NH_3 in MeOH, 70–90%; (f) $POCl_3$, DIPEA, 1,2-dichloroethane, reflux then; (g) 3-chloro-4-fluoroaniline, DIPEA, IPA, reflux, 20–70% two steps.

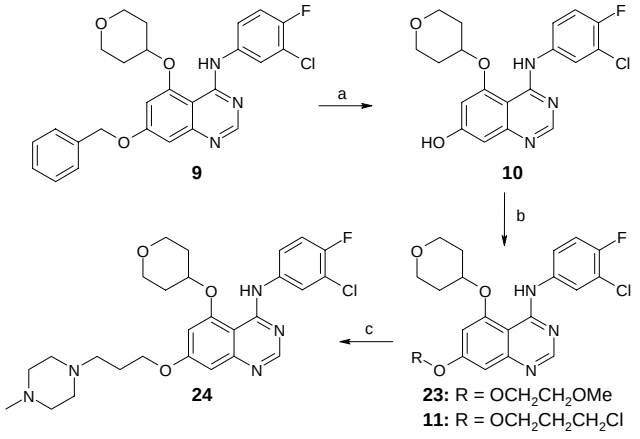

Scheme 2. Synthesis of 5,7-bisalkoxy anilinoquinazolines **23** and **24**. Reagents and conditions: (a) TFA, 70 °C, 82%; (b) K_2CO_3, DMF, R-Br, 77–78%; (c) 1-methyl piperazine, NMP, 80 °C.

Biological data for representative compounds is highlighted in Table 1.[15] Positioning of a cyclic, basic group at C-5 such as the *N*-methylpiperidine **12** resulted in potent enzyme inhibition. Cyclic groups that lacked this charge tended to show lower affinity. Tetrahydropyran **13**, for example, shows significantly decreased inhibition, although tetrahydrofuran **14** demonstrates a more modest drop compared to **13**, perhaps reflecting the greater structural similarity to the sugar it is designed to mimic. Figure 1 (upper panel) shows the anticipated binding mode for **12** docked into the EGFR tyrosine kinase structure. A conformational ensemble for **12** generated in OMEGA had the anilinoquinazoline moiety overlaid with that of *erlotinib* and the resulting poses scored using the Poisson–Boltzmann equation based ZAP.[16] The protein surface is coloured according to electrostatic potential.[17] The ribose pocket is characterised as having substantially negative surface potential, and it is speculated that the high affinity seen for basic groups in this region may be due to electrostatic complementarities with the cationic side chain. The reduced activity observed with open-chain *iso*-propyl analogue **15** serves to highlight the importance of cyclic groups in this region.

Table 1. EGFR inhibition data for compounds **12–24**

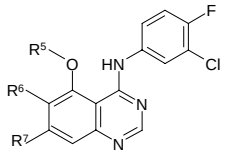

Compound	R^5	R^6	R^7	EGFR IC_{50} (nM)[a]
12	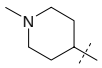	H	MeO	21 ± 3
13		H	MeO	1384 ± 150
14		H	MeO	187 ± 77
15		H	MeO	8068
16	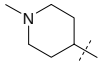	MeO	H	225 ± 50
17	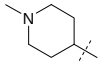	H	H	3 ± 2
18		H	MeO	10 ± 1
19	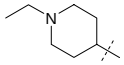	H	MeO	<2[b]
20	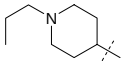	H	MeO	<2[b]
21	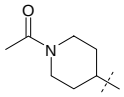	H	MeO	873
22	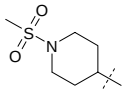	H	MeO	9601
23		H	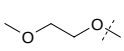	671 ± 35
24		H	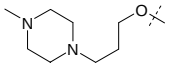	66 ± 22

[a] For determinations where $n \geqslant 2$, standard deviation is given.
[b] $n = 2$, lower than assay limit.

Table 2. Selected DMPK data for compound **12**

	PPB free %[a]	V_{dss} (L/kg)	Cl (ml/min/kg)	$t^{1/2}$ (h)	Bio-availability (%)
Mouse	3.11	8.2	20	5.2	103
Rat	2.51	12.3	66	2.9	63

[a] Measured at 37 °C (mouse) and 25 °C (rat).

Compound **16** illustrates that moving the methoxy group to C-6 results in an order of magnitude drop in affinity when compared with **12**, and this may be due to a significant conformational change in the C-5 side chain. Removal of the methoxy group as in **17** also leads to a potent inhibitor, although in general terms, removal of the C-7 methoxy was often seen to be detrimental to EGFR inhibition (when a broader range of anilines was examined, the mean change in activity from C-7 hydrogen to C-7 methoxy is a potency shift of 1.2 log units, 14 matched pairs, data not shown). We next examined the effect of extension from the basic nitrogen in **12**. Consistent with the binding model, the N–H piperidine analogue **18** showed similar affinity to the *N*-methyl analogue **12**. Introduction of ethyl (compound **19**) and propyl (compound **20**) also resulted in potent enzyme inhibition, indicating a degree of tolerance for steric bulk in this region. Consistent with the hypothesised charge interaction around the ribose binding pocket, neutral piperidines such as **21** and **22** showed markedly reduced activity. Finally, we observed that by use of a suitably positioned basic side chain at C-7, activity could be regained with a previously less active C-5 substituent. Tetrahydropyran **13** demonstrates modest affinity as discussed above. By appending the piperazine-based side chain in **24**, activity is restored and potent inhibition seen. Figure 1 (lower panel) shows this compound docked into EGFR tyrosine kinase. In this model, the C-5 tetrahydropyran occupies the ribose binding pocket, and the basic C-7 side chain extends towards the solvent exposed region and may pick up favourable charge interactions in the area towards Glu780. That this is likely due to charge complementarities is supported by compound **23** that positions a neutral side chain at C-7 yet shows a similarly low affinity to tetrahydropyran **13**.

Compound **12** was selected for further study. In an EGF-driven KB cell proliferation assay,[15] **12** was shown to inhibit proliferation with an IC_{50} of 87(±4) nM. Selected DMPK data are shown in Table 2 following an oral dose of 5 mg/kg and iv dose of 2 mg/kg. A good pharmacokinetic profile were observed in both mouse and rat, with data superior in the former. Slightly higher clearance and a shorter half-life was observed in the rat compared with mouse, and consistent with the presence of a basic side chain, V_{dss} was seen to be high in both species. Solubility in pH 7.4 buffer was measured at 2.1 μM. Based on the observed potency in cell-based assays, and the favourable pharmacokinetic profile, compound **12** was progressed to a LoVo Xenograft study (Fig. 2). Female nude mice were implanted subcutaneously with 1×10^7 LoVo colon tumour cells. Once tumours were established, animals were randomised between groups ($n = 7$ per group) and dosed once daily

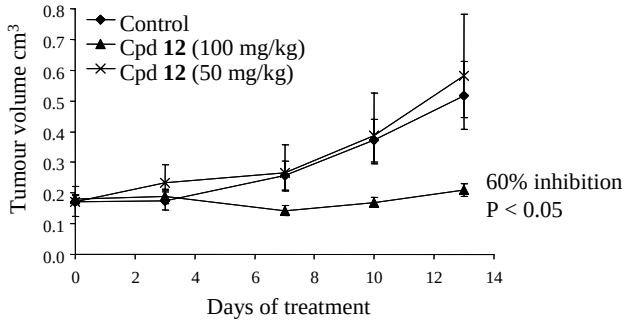

Figure 2. LoVo xenograft study with compound **12** showing degree of inhibition of tumour volume after 13 days of treatment. Terminal blood samples were taken 6 h after the final dose and analysis showed a dose related increase in total exposure: 2.3 μM (50 mg/kg) and 4.1 μM (100 mg/kg).

po with compound suspended in 1% (v/v) polysorbate 80. Tumour growth was measured twice-weekly using callipers. Gratifyingly at the highest dose tested, 100 mg/kg, compound **12** demonstrated 60% inhibition of tumour volume. A clear dose response was observed, with no significant change from control seen at the lower dose of 50 mg/kg.

In summary, chemistry has been developed to a series of novel C-5 substituted anilinoquinazolines, selected on the basis of docking experiments and overlays with ATP in the active site of EGFR tyrosine kinase. Clear SAR emerged concerning the requirements for good affinity with these structures, in particular the requirements for basic moieties at positions C-5 and/or C-7. Selected examples exhibit both good cellular activity and pharmacokinetics, and resulted in significant inhibition in an in vivo model of anti-cancer activity.

References and notes

1. Yarden, Y.; Sliwkowski, M. X. *Nat. Rev. Mol. Cell Biol.* **2001**, *2*, 127.
2. Salomon, D. S.; Brandt, R.; Ciardiello, F.; Normanno, N. *Crit. Rev. Oncol. Haematol.* **1995**, *19*, 183.
3. Herbst, R. S.; Fukuoka, M.; Baselga, J. *Nat. Rev. Cancer* **2004**, *4*, 956.
4. Bonomi, P. *Expert Opin. Investig. Drugs* **2003**, *12*, 1395.
5. Douglas Laird, A.; Cherrington, J. M. *Expert Opin. Investig. Drugs* **2003**, *12*, 51; Ciardiello, F.; De Vita, F.; Orditura, M.; De Placido, S.; Tortora, G. *Expert Opin. Emerg. Drugs* **2003**, *8*, 501.
6. (a) Rewcastle, G. W.; Denny, W. A.; Bridges, A. J.; Zhou, H.; Cody, D. R.; McMichael, A.; Fry, D. W. *J. Med. Chem.* **1995**, *38*, 3482; Bridges, A. J.; Zhou, H.; Cody, D. R.; Rewcastle, G. W.; McMichael, A.; Showalter, H. D. H.; Fry, D. W.; Kraker, A. J.; Denny, W. A. *J. Med. Chem.* **1996**, *39*, 267.

7. Maria, G. C. *IDrugs* **2004**, *7*, 58.
8. Stamos, J.; Sliwkowski, M. X.; Eigenbrot, C. *J. Biol. Chem.* **2002**, *277*, 46265.
9. Wood, E. R.; Truesdale, A. T.; McDonald, O. B.; Yuan, D.; Hassell, A.; Dickerson, S. H.; Ellis, B.; Pennisi, C.; Horne, E.; Lackey, K.; Alligood, K. J.; Rusnak, D. W.; Gilmer, T. M.; Shewchuk, L. *Cancer Res.* **2004**, *64*, 6652.
10. Shewchuk, L.; Hassell, A.; Wisely, B.; Rocque, W.; Holmes, W.; Veal, J.; Kuyper, L. F. *J. Med. Chem.* **2000**, *43*, 133.
11. Barker, A. J.; Gibson, K. H.; Grundy, W.; Godfrey, A. A.; Barlow, J. J.; Healy, M. P.; Woodburn, J. R.; Ashton, S. E.; Curry, B. J.; Scarlett, L.; Henthorn, L.; Richards, L. *Bioorg. Med. Chem. Lett.* **2001**, *11*, 1911.
12. Hou, T.; Zhu, L.; Chen, L.; Xu, X. *J. Chem. Inf. Comput. Sci.* **2003**, *43*, 273.
13. For the first disclosure of C-5 substituted anilinoquinazolines see Hennequin, L.F.A.; Ple, P. PCT Int. Appl. WO2001094341; For a related series targeting erbB2 tyrosine kinase see: Ballard, P.; Bradbury, R. H.; Hennequin, L. F. A.; Hickinson, D. M.; Johnson, P. D.; Kettle, J. G.; Klinowska, T.; Morgentin, R.; Ogilvie, D. J.; Olivier, A. *Bioorg. Med. Chem. Lett.* **2005**, *15*, 4226.
14. Hennequin, L. F.; Allen, J.; Costello, G. C.; Curwen, J.; Fennell, M.; Green, T. P.; Jacobs, V.; Lambert-van der Brempt, C.; Morgentin, R.; Olivier, A.; Ple, P. A.; Whittaker, R. Structure–activity relationship and in vivo activity of a novel series of C5-substituted anilinoquinazolines with highly potent and selective inhibition of c-Src tyrosine kinase activity. Proc. Am. Assoc. Cancer Res. 2003. Abstract B193.
15. Compounds were evaluated in an EGFR kinase assay measuring inhibition of phosphorylation of a synthetic peptide substrate at K_m ATP concentration, and their ability to inhibit growth of the KB cell line when stimulated with EGF assessed. For details of assay conditions, see Hennequin, L. F. A.; Kettle, J. G.; Pass, M.; Bradbury, R. H. PCT Int. Appl. WO2003040109.
16. OMEGA and ZAP are available from OpenEye Scientific Software, 3600 Cerrillos Rd., Suite 1107, Santa Fe, NM 87507.
17. Images created in Pymol: Delano, W. L. *The Pymol Molecular Graphics System*; Delano Scientific LLC, San Carlos, CA, USA Baker, N. A.; Sept, D.; Joseph, S.; Holst, M. J.; McCammon, J. A. *Proc. Natl. Acad. Sci. U.S.A.* **2001**, *98*, 10037.